ENDF/B-VIII.1-Based DeCART2D Multi-Group Cross-Section Library Generation with Proposed Correction Order Selection Procedure

Jeongkyu Cho [a] and Ho Jin Park [a*]
a Kyung Hee University, 1732 Deokyoungdaero, Giheung-gu, Yongin-Si, Gyeonggi-do, Korea, 17104
[*]Corresponding author: parkhj@khu.ac.kr

***Keywords :** DeCART2D, ENDF/B-VIII.1, McCARD, Library Correction, APR-1400 Benchmark

1. Introduction

The DeCART2D lattice transport code [1] requires a multi-group (MG) cross-section library, which is generated by the KAERI (Korea Atomic Energy Research Institute) library generation system [2] from an evaluated nuclear data library. Because the DeCART2D MG library relies on an approximate neutron spectrum for neutron energy-group collapse, DeCART2D calculations yield results that differ from continuous-energy Monte Carlo (MC) reference solutions. To reduce DeCART2D errors that arise from the approximations employed in library generation, Kim and Park [2–3] investigated the application of group-wise correction factors and established the library correction system. Each correction factor was defined as the ratio of the MC reference reaction rate to the DeCART2D reaction rate for a specific nuclide, reaction, energy group, and temperature. The correction process continues until the correction factors converge, with the McCARD continuous energy Monte Carlo transport code [4] as the reference solution.

Although correction factors can be generated at relatively low computational cost, simultaneous correction of multiple nuclides may introduce additional errors because cross-section changes for different nuclides can interfere with one another through their effects on the neutron spectrum. Therefore, this study identifies which nuclides and temperatures require priority correction to minimize the final error. We refer to this procedure as "correction order selection procedure".

In this study, the convergence of Gd reaction rates under the simultaneous correction of multiple nuclides was analyzed to produce an ENDF/B-VIII.1-based DeCART2D library. The cause of the non-monotonic behavior was then identified, and a staged correction procedure was applied. Finally, the corrected library was evaluated with APR-1400 benchmark problems.

2. ENDF/B-VIII.1 DeCART2D Library Generation and Correction Order Selection Procedure

The Kyung Hee University (KHU) library correction system [2-3] was incorporated into the KAERI library generation system to generate group-wise correction factors from the ratios of the MC reaction rates to the corresponding DeCART2D reaction rates. For nuclide i, reaction x, energy group g, and temperature T, the factor is

$$f_{x,g,i}^{(n+1)}(T) = \frac{\sigma_{x,g,i}^{MC}(T) \cdot \phi_g^{MC}(T)}{\sigma_{x,g,i}^{De}(T) \cdot \phi_g^{De}(T)} \quad \ldots(1)$$

where σ and ϕ are the microscopic cross section and the neutron flux, and "MC" and "De" superscripts denote McCARD and DeCART2D, respectively. To generate a DeCART2D library for typical PWR analyses, the APR-1400 B3 fuel assembly (FA) with a boron concentration of 1000 ppm was selected as the base model for correction-factor calculation. Correction factors were calculated for the applicable absorption, fission, and scattering reactions of ^{235}U, ^{238}U, ^{1}H, ^{10}B and $^{154-160}$Gd. The correction process continued until the DeCART2D reaction rates agreed with the MC reference values. Moreover, the $^{1}H_{ref}$ and $^{10}B_{ref}$ isotopes in the reflector region at the core periphery were corrected by solving a 3-node problem, which consists of one normal FA (C0-type) and two reflector blocks including the shroud.

Under simultaneous correction, cross section changes in one nuclide alter the neutron flux and the reaction rates of other nuclides; thus, the coupled reaction rates may not converge monotonically. The Gd reaction rate showed a pronounced non-monotonic response. Two correction options were compared to assess the effect of correction order. Fig. 1 compares the Gd-first option (Gd corrected first, followed by all nuclides) with the U-first option (^{235}U and ^{238}U corrected first, followed by all nuclides) results in terms of the ^{155}Gd reaction-rate RMS error at 300K.

In the Gd-first option, correction is performed on the Gd absorption reaction to converge the reaction rate difference of Gd, and then correction is performed also with other nuclides. In the U-first option, correction is performed on the U absorption reaction to converge the reaction rate difference of U, and then correction is performed also with other nuclides. In both options, the correction factors at each round are recalculated using the reaction rates obtained with the library generated in the preceding round, starting from the uncorrected ENDF/B-VIII.1 library (UCR).

Under the Gd-first option, the RMS error of Gd-155 300K resonance group's reaction rate difference is driven below 0.1% and then rebounds to 1.4% when other nuclide's correction starts. Under the U-first option, the Gd difference decreases monotonically to 0.46% without a rebound. Both options eventually approach similar RMS errors; thus, the principal difference lies in

the convergence path rather than the final level of agreement. To identify the source of the Gd perturbation, additional isolation calculations were performed by applying the correction to one reaction or nuclide at a time. Among the tested cases, the uranium absorption correction produced the dominant perturbation in the Gd reaction rate, whereas the uranium fission and other nuclide corrections produced only minor changes. These tests indicate that the non-monotonic Gd response is primarily caused by the uranium absorption correction.

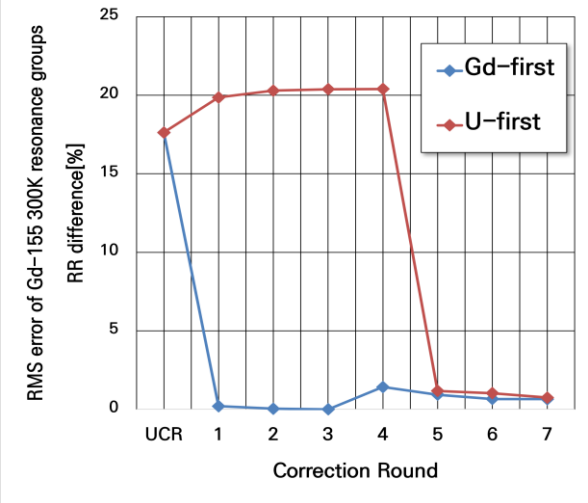


Fig. 1(a). RMS error of the ^{155}Gd reaction-rate differences over resonance groups at 300K for the Gd-first and U-first correction options.

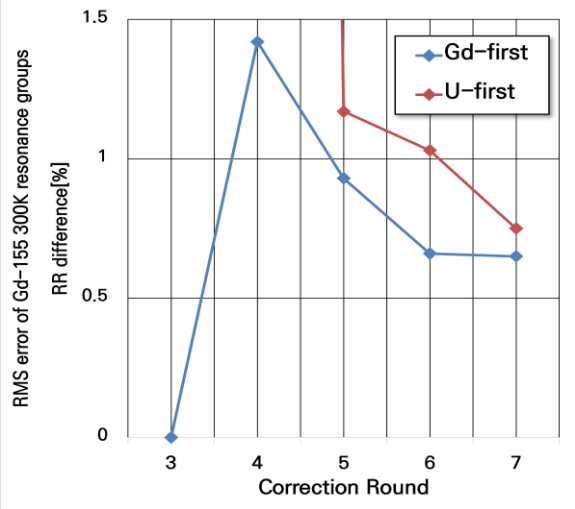


Fig. 1(b). Enlarged view of the ^{155}Gd reaction-rate differences over resonance groups at 300K

This behavior can be explained by the strong spectrum coupling between uranium and Gd. The ^{238}U resonance absorption shapes the epithermal flux and the slowing down of neutrons into the thermal range, where the Gd reaction rate is highly sensitive to the neutron spectrum. Consequently, updating the ^{235}U and ^{238}U absorption cross sections redistributes the neutron flux and perturbs the Gd reaction rate, even when Gd is corrected in the same round. Uranium absorption acts as a dominant spectral driver for the Gd reaction rate, and stabilizing the uranium-driven spectrum before correcting Gd avoids the rebound observed in the Gd-first option. Although both correction options approach similar reaction rates for the reference assembly, the U-first option provides a more stable convergence path. Therefore, the U-first option is adopted as the baseline correction option for the correction order selection procedure. The correction order selection procedure is designed to separate the correction of the dominant spectral driver from that of the remaining nuclides. During the initial correction stage, the uranium absorption cross sections are corrected while the other nuclides are held unchanged, so that the major change in the fuel neutron spectrum is established before the Gd cross sections are adjusted. During the correction stage 1, correction of uranium, the principal fissile isotope in a commercial PWR system, substantially reduces the reactivity error relative to the uncorrected case. However, because this stage corrects only the uranium cross sections, the reactivity and reaction-rate errors associated with other nuclides (i.e., B, H, and Gd) remain nearly unchanged. Therefore, correction stage 1 primarily serves to stabilize the overall neutron spectrum.

Based on these results, two correction stages were established. In the correction stage 1 (R1–R4), only the ^{235}U and ^{238}U absorption cross sections were corrected until the uranium resonance reaction rates converge. In the correction stage 2 (R5–R9), the correction was extended to all selected nuclides and reactions, allowing the remaining reaction-rate differences to converge under the uranium-adjusted spectrum. After these two stages (R1–R9), APR-1400 benchmark calculations were performed to assess the accuracy of the correction stage 2 (R9) library and determine whether further correction was required. Table I summarizes the correction target, temperature range, and purpose of each correction stage. Section 3.1 will give the detail explanation for the correction stage 3 with APR-1400 benchmark validation analyses.

Table I: Correction stages for ENDF/B-VIII.1 47-group DeCART2D library generation

Correction Stage	Round	Correction Target		Purpose
		Nuclide and reaction	Temp*	
1	R1-R4	Uranium capture and fission	All	Stabilize U-driven Spectrum
2	R5-R9	All nuclides and reactions	All	Converge the coupled reaction rates
3	R10-R13	All nuclides and reactions	CZP	Reduce the localized CZP residual

* Temperature : CZP, HZP, HFP, All (CZP+HZP+HFP)
** Cold Zero Power (CZP), Hot zero Power (HZP), Hot full Power (HFP)

3. APR-1400 Benchmark Evaluation of the Newly Generated ENDF/B-VIII.1 DeCART2D Library

The new ENDF/B-VIII.1 DeCART2D libraries generated via the correction order selection procedure were evaluated using the APR-1400 benchmark problems [5,6] and compared with McCARD [4] reference solutions. The APR-1400 benchmark core consists of 241 FAs arranged within a 17×17 core lattice, with each FA containing 236 fuel rods. Table II summarizes the benchmark problems: single pin (45), 2D FA (81), and 2D core (9). Problem conditions combine the operating state—Cold Zero Power (CZP), Hot Zero Power (HZP), or Hot Full Power (HFP)—with boron levels of 0, 1000, and 2000 ppm.

Table II: Summary of APR-1400 Benchmark problems

No.	Problem type	Conditions summary
1	Single pin	5 enrichments, 3 temperature points 3 boron levels
2	2D FA	9 assemblies, 3 temperature points, 3 boron levels
3	2D core	3 temperature points, 3 boron levels

The RMS errors of reactivity between DeCART2D and the reference are evaluated separately for the single pin, FA, and 2D core problems. With the uncorrected library (UCR), the RMS errors are 537, 692, and 629 pcm respectively. During the correction stage 1 (R1–R4), only the uranium absorption (i.e, capture and fission reaction) cross sections are corrected. Consequently, the RMS error in reactivity decreases, whereas the RMS error in the Gd reaction rate remains nearly unchanged because the Gd cross sections have not yet been corrected. The goal of this stage is to stabilize the uranium-driven neutron spectrum before the coupled correction is applied to the remaining nuclides and reactions. The errors decrease in the correction stage 2 (rounds R5–R9), where all selected nuclides and reactions are corrected, reaching 63, 111, and 62 pcm for the single pin, 2D FA, and 2D core problems. The remaining condition-dependent errors are examined below to determine whether an additional Correction stage is necessary.

3.1 Cold Zero Power(CZP) condition correction and overfitting

After the two correction stages (R1–R9), the correction stage 2 (R9) library is assessed with the APR-1400 benchmark to decide whether further correction was required. Although the overall reactivity errors were already greatly reduced, a localized residual remained under the cold condition. To remove it, the correction stage 3 (R10–R12) was introduced, in which the correction was restricted to the cold-temperature (CZP) condition while the hot conditions were left unchanged because their reaction rates had already converged in the correction stage 2. This subsection first identifies the R9 condition-dependent residual that motivates the correction stage 3, and then examines the correction stage 3 (R12) library and the correction stage 3+ (R13) library results, including the onset of overfitting. The correction stage 3+ (R13) which is corrected from R12 library was also restricted to correct under the CZP condition.

Table III summarizes the condition-dependent reactivity RMS errors at the correction stage 2 (R9), the correction stage 3 (R12), and correction stage 3+ (R13). At the correction stage 2 (R9), the largest residual is observed for the CZP FA problems with Gd pins (222 pcm), whereas the CZP pin problems (73 pcm), CZP FA problems without Gd pins (28 pcm), and HZP+HFP FA problems with Gd pins (44 pcm) already show much smaller errors. This localized residual motivates an additional correction stage targeted at the cold condition; the correction stage 3 and the correction stage 3+ (R13) results are discussed below.

Table III: RMS Error of Reactivity (pcm) by APR-1400 Benchmark Problem Group and Condition

Problem	Correction stage 2	Correction stage 3	Correction stage 3+*
CZP FA with Gd pins (18)	222	140	102
CZP pin (15)	73	68	93
CZP FA w/o Gd pin (9)	28	36	62
HZP+HFP FA with Gd pins (36)	44	44	45

* An additional correction round was performed to assess potential overfitting.

In the correction stage 3, the correction is restricted to the CZP conditions, while no further correction is applied at the hot conditions because their reaction rates had already converged in the correction stage 2. The RMS error for the CZP FA problems with Gd pins decreases from 222 pcm at the correction stage 2 to 140 pcm at the correction stage 3; the errors for the CZP pin and FA without Gd problems remain relatively small at 68 and 36 pcm, respectively, and the RMS error of the HZP+HFP FA problems remains 44 pcm. The overall pin, 2D FA, and 2D core RMS errors at the correction stage 3 are 61, 77, and 49 pcm, respectively. When the cold-only correction is continued to R13, the CZP Gd assembly error decreases further to 102 pcm, but the errors of the CZP pin and CZP non-Gd assemblies increase to 93 and 62 pcm, respectively. Because the improvement is limited to the corrected Gd assemblies while the other cold problems become worse, this behavior indicates overfitting to the reference model and the correction is therefore stopped at the correction stage 3. The resulting library is denoted the correction stage 3 and is used as the corrected library in this study. Fig. 2 summarizes the complete three-stage correction procedure.

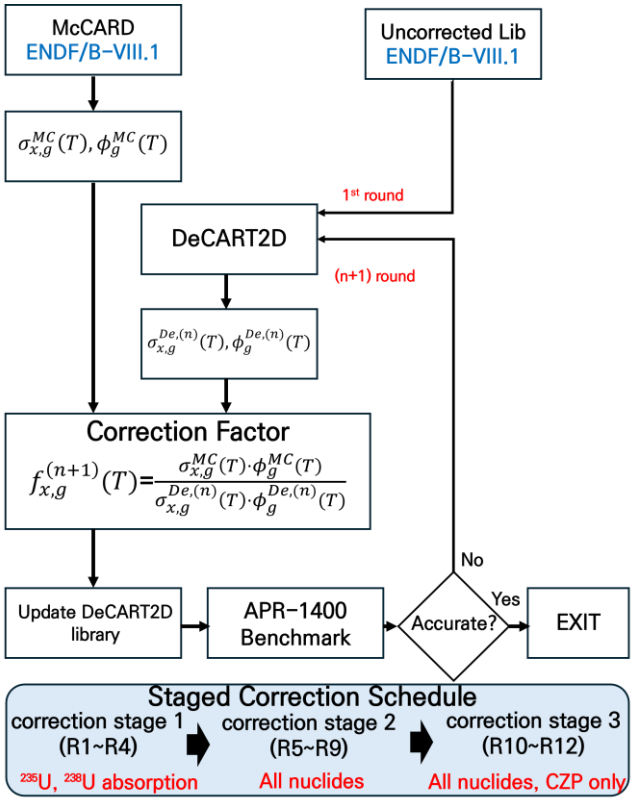


Fig. 2. Staged library correction procedure

Table IV compares the RMS errors of Reactivity for the uncorrected library (UCR), correction stage 2 library, and the correction stage 3 library. At the correction stage 2, the single pin, 2D FA, and 2D core RMS errors of Reactivity are 63, 111, and 62 pcm, respectively. The cold-only correction in the correction stage 3 further reduces the 2D FA and 2D core RMS errors to 77 and 49 pcm, while the single pin error decreases slightly to 61 pcm.

Table IV: RMS error of reactivity (pcm) for the UCR, correction stage 2, and correction stage 3 libraries

Problem	Uncorrected (UCR)	Correction stage 2	Correction stage 3
Single Pin(45)	537	63	61
2D FA(81)	692	111	77
2D core(9)	629	62	49

Figure 3-5 show the results of single pin, 2D FA and 2D core problem for each Problem ID. Problem IDs of Figure 3 and 4 are assigned by combining the operating condition Cold Zero Power (CZP), Hot Zero Power (HZP), or Hot Full Power (HFP) with the boron concentration level: '0' for 0 ppm, '1' for 1000 ppm, and '2' for 2000 ppm. And Problem ID of Figure 4 is based on enrichment and the presence of gadolinium (Gd) burnable absorbers, nine FA types are defined: A0, B0-B3, and C0-C3.

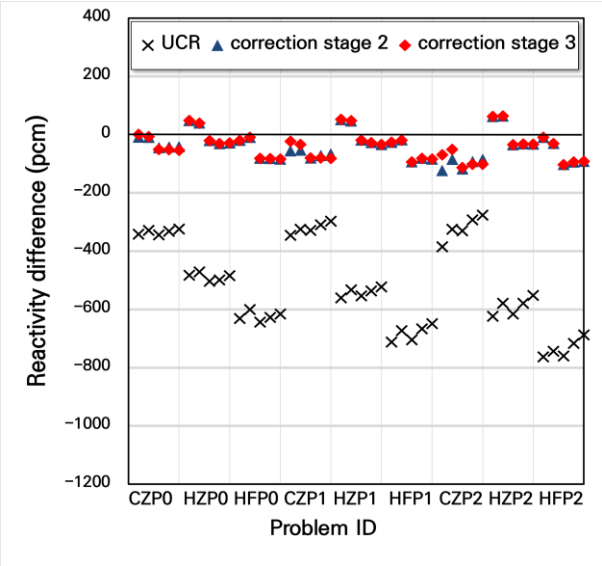


Fig. 3. Reactivity errors for the Single Pin problems

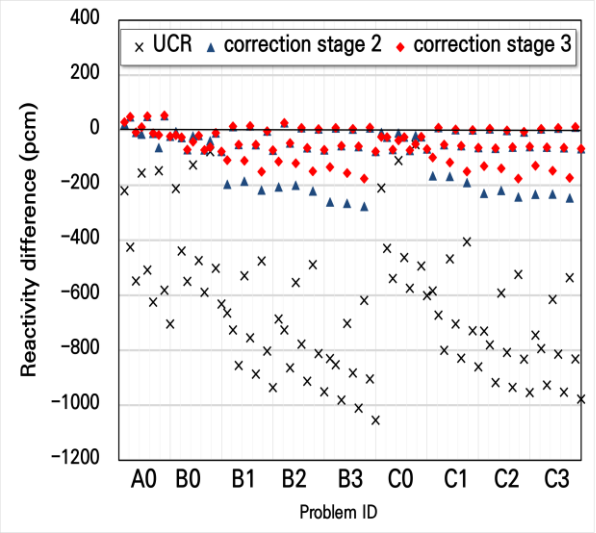


Fig. 4. Reactivity errors for the 2D FA problems

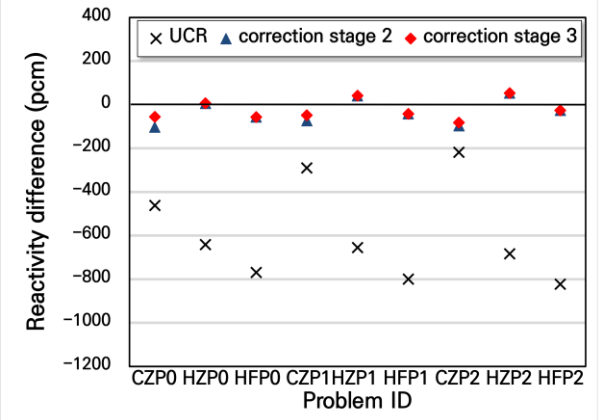


Fig. 5. Reactivity errors for the 2D core problems

3.2 Errors in pin-wise power distributions for 2D FA problems

Fig. 6 presents the pin power distribution errors for the 2D FA benchmark problems obtained with each library. The average RMS errors are 0.21%, 0.15%, and 0.15% for the UCR, correction stage 2, and the correction stage 3 libraries, respectively. These results indicate that the reactivity improvement obtained through the library correction is accompanied by improved prediction of the local pin-power distribution, while the additional cold-only correction from the correction stage 2 library to the correction stage 3 has little effect on the overall pin-power distribution.

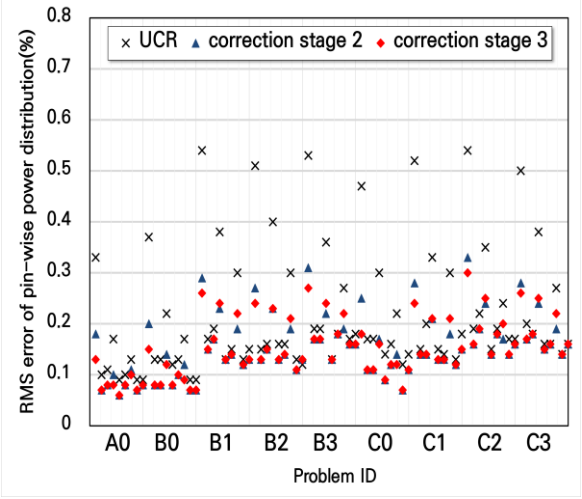


Fig. 6. Comparison of pin-wise power-distribution RMS errors for 2D FA problems

3.3 Errors in assembly-wise power distributions for 2D core problems

Fig.7 presents the assembly power distribution errors for the 2D core benchmark problems obtained with each library. The average RMS errors are 2.19%, 1.48% and 1.29% for the UCR, correction stage 2, and the correction stage 3 libraries, respectively.

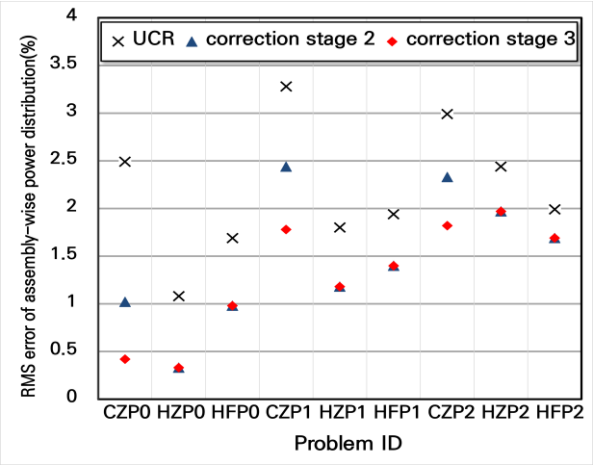


Fig. 7. Comparison of assembly-wise power-distribution RMS errors for 2D core problems

4. Conclusion

In this study, an ENDF/B-VIII.1-based 47 group DeCART2D library was newly generated and corrected by the correction order selection procedure. This correction order selection procedure was developed to determine the correction option (i.e., U-first or Gd-first) and minimize cross-section coupling effects. Various analyses were performed to determine the correction priority between U and Gd, which have the greatest influence on PWR reactivity. Based on the results, the "U-first" option was selected. APR-1400 benchmark calculations were then performed to assess the performance of the corrected library – the correction stage 2 library.

For the APR-1400 benchmark, the correction stage 2 library reduced the single pin, 2D FA, and 2D core reactivity RMS errors from 537, 692, and 629 pcm with the uncorrected library (i.e., UCR) to 63, 111, and 62 pcm, respectively. The average pin power distribution RMS error decreased from 0.21% with the uncorrected library to 0.15% at the correction stage 2 and remained unchanged at the correction stage 3. The average assembly power distribution RMS error decreased from 2.19% with the uncorrected library to 1.48% at the correction stage 2 and reduced to 1.29% at the correction stage 3. The subsequent cold-only the correction stage 3 library reduced the CZP FA RMS error to 140 pcm and the overall single pin, 2D FA, and 2D core reactivity RMS errors to 61, 77, and 49 pcm at the correction stage 3 (i.e., R12) library, respectively. Moreover, the additional correction round (i.e., R13) was performed to assess potential overfitting. However, extension to R13 caused overfitting.

Future work will aim to reduce the required correction rounds and establish improved termination criteria and correction options.

Acknowledgment

This work was supported by the National Research Foundation of Korea (NRF) grant funded by the Korea government (Ministry of Science and ICT) (No. RS-2024-00422848).

REFERENCES

[1] J. Y. Cho et al., "DeCART2D v1.1 User's Manual," KAERI/UM-40/2016, 2016.
[2] H. J. Park et al., "An improved DeCART library generation procedure with explicit resonance interference using continuous energy Monte Carlo calculation," Ann. Nucl. Eng., 105, pp. 95–105, 2017.
[3] C. Kim and H. J. Park, "Improvement of DeCART2D multigroup cross section library correction system and APR-1400 benchmarking," Nucl. Eng. Technol., 57, 103820, 2025.
[4] H. J. Shim et al., "McCARD: Monte Carlo Code for Advanced Reactor Design and Analysis," Nucl. Eng. Technol., 44, pp. 151–176, 2012.

[5] S. Yuk, "APR1400 Reactor Core Benchmark Problem Book," Technical Report RPL-INERI-CA-004, KAERI, Daejeon, South Korea, 2019.
[6] C. Kim and H. J. Park, "DeCART2D Calculations of APR-1400 Benchmark using Improved Cross Section Library Generation System," International Conference on Mathematics and Computational Methods Applied to Nuclear Science and Engineering (M&C 2025), Denver, CO, April 27–30, 2025.